ARMY RESEARCH LABORATORY

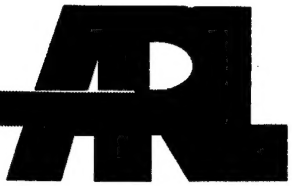

Yaw Card Perturbation of Projectile Dynamics

Gene R. Cooper
Kevin S. Fansler

ARL-TR-1258

JANUARY 1997

The findings in this report are not to be construed as an official Department of the Army position unless so designated by other authorized documents.

Citation of manufacturer's or trade names does not constitute an official endorsement or approval of the use thereof.

Destroy this report when it is no longer needed. Do not return it to the originator.

Army Research Laboratory
Aberdeen Proving Ground, MD 21005-5425

ARL-TR-1258 January 1997

Yaw Card Perturbation of Projectile Dynamics

Gene R. Cooper
Kevin S. Fansler
Weapons & Materials Research Directorate

Abstract

Projectile flight through a yaw card range is investigated with particular attention given to the apparent change in the flight coefficients. Encounters of the projectile with the yaw cards are treated as impulses, resulting in calculated abrupt changes in the yaw modal arms' phases and amplitudes. Further approximations are made to describe small perturbing encounters and to obtain an expression for the apparent or range value for the overturning moment coefficient. For 7.62-mm ammunition, apparent flight coefficients are calculated point by point for various yaw card spacings and compared with simple approximating expressions. Resonance conditions are also investigated, whereby the yawing motion of a spin-stabilized projectile can be amplified. These resonance conditions force the amplitude ratio for the fast and slow modal arms toward unity and the encountering phase angle of the projectile toward a value that maximizes the amplification for each encounter.

ACKNOWLEDGMENTS

We wish to thank Mr. Robert McCoy for his comments and suggestions to improve this work. We also thank Mr. Vural Oskay for his technical review of this report.

INTENTIONALLY LEFT BLANK.

TABLE OF CONTENTS

INTENTIONALLY LEFT BLANK.

LIST OF FIGURES

INTENTIONALLY LEFT BLANK.

LIST OF TABLES

INTENTIONALLY LEFT BLANK.

YAW CARD PERTURBATION OF PROJECTILE DYNAMICS

1. INTRODUCTION

Spark photography ranges have largely replaced yaw card ranges to obtain projectile flight coefficients (Braun 1958; Kittyle, Packard, and Winchenbach 1987). Spark photography ranges yield higher measurement accuracy, no interference with the projectile's flight, and high quality flow field visualization. Nevertheless, yaw card testing is still used for various reasons (Boyer 1963; McCoy 1992); yaw card testing is less expensive, yields results more quickly, avoids spark range damage from discarding projectile parts, and permits toxic or hazardous materials to be tested in an open air facility rather than the closed environment of a spark range.

The free flight coefficients obtained by spark ranges and yaw card ranges usually differ in value by a small but significant amount. This difference is caused by the projectile's physical interaction with the yaw card material. Other investigators have attempted to correct the yaw card results by either empirical means or methods based on theory (Boyer 1963; Hitchcock 1941, 1942, 1953; Karpov 1953). McCoy (1992) recently presented a theoretical explanation for the free flight coefficient values observed in a yaw card range. He represents these cards as small segments in the projectile's path with different flight coefficients. With the assumption of a uniformly spaced array, McCoy (1992) obtains a small additive term to the usual pitching moment coefficient value, discussed extensively by McShane, Kelley, and Reno (1953). This small additive term depends upon the yaw card spacing and the physical properties of the yaw cards. Confirmation of the theory is obtained by reduction of the firing data, which shows that the measured overturning moment coefficient depends on the card spacings. This functional dependence of the moment coefficient on the card spacing can be used to extrapolate the values obtained by a spark range. The extrapolated value of the aerodynamic pitching moment coefficient agreed within 2% with the results obtained in an aerodynamic spark range (McCoy 1988).

However, each encounter of the projectile with a yaw card changes the epicyclic motion, possibly increasing or decreasing the magnitude of the precessing and nutation arms. The phase values for the epicycles will also be changed by the interaction as already determined by McCoy (1992). If a uniform spacing is chosen in the stable regime, the phase values fluctuate within an envelope. It is a goal of this work to present a theory of yaw card interactions that more accurately describes the particular projectile interactions at each card location.

In this work, interactions with the yaw cards are treated as discrete impulses. The corresponding differential equation describing the pitching and yawing motion has added terms containing the Dirac delta function (Dennery and Krzywicki 1967). Integration of the resulting differential equation through a yaw card yields difference equations whose solution gives the change in the phase and amplitude of the usual two mode yawing motion of a free flight projectile. Yaw cards spaced uniformly are treated and the conditions for increasing yaw amplitude are presented and discussed.

2. YAW CARD MOMENTS AND IMPULSES

The equivalent aerodynamic overturning moment for a projectile passing through card material is simply a specialization of the usual aerodynamic definition to the card material:

$$M_{M_c} = \frac{\pi}{4}\rho_c d^3 V^2 C_{M_{\alpha c}} \sin\alpha_t, \tag{1}$$

in which

$$\begin{aligned} C_{M_{\alpha c}} &= \text{moment overturning coefficient for card material} \\ \rho_c &= \text{density of card material} \\ d &= \text{projectile reference diameter} \\ V &= \text{speed of projectile at impact with card} \\ \alpha_t &= (\alpha^2+\beta^2)^{\frac{1}{2}}, \text{total angle of attack} \\ \alpha &= \text{angle of attack} \\ \beta &= \text{angle of side slip.} \end{aligned}$$

The corresponding drag and normal force values are expressed as usual so that the subscript c denotes the card material. These equivalent coefficients depend upon the density of the material, card thickness, projectile geometry, and so forth.

When the projectile transits a yaw card, the forces and moments occur for such a short time that the event can be treated as an impulse, whose magnitude depends upon the thickness of the yaw card, τ_c. The card overturning moment impulse, imparted by the yaw card to the projectile, is M_{Mc} multiplied by a characteristic time of interaction, $\Delta t = \tau_c/V$, which is

$$\mathcal{I}_{M_c} = \frac{\pi}{4}\rho_c d^3 \tau_c V C_{M_{\alpha c}} \sin\alpha_t. \tag{2}$$

3. THE DIFFERENTIAL EQUATION OF MOTION FOR A PROJECTILE FIRED THROUGH YAW CARDS

Equation (1), when used with Newton's second law, is the starting point for developing the differential equation of pitching and yawing motion for a spinning, symmetrical projectile. With further considerations, such as assuming a linear pitching moment and neglecting damping processes, it is obtained that a differential equation involving the independent variable of distance in calibers is, in Murphy's notation (1963),

$$\tilde{\xi}'' - iP\tilde{\xi}' - M\tilde{\xi} = 0, \tag{3}$$

in which

$$\begin{aligned}
\tilde{\xi} &\approx \sin\beta + i\sin\alpha, \text{the complex yaw} \\
P &= \frac{I_x}{I_y}\frac{pd}{V} \\
M &= \frac{\rho S d^3}{2I_y} C_{M_\alpha} \\
I_x &= \text{axial moment of inertia} \\
I_y &= \text{transverse moment of inertia} \\
p &= \text{axial spin} \\
\rho &= \text{air density} \\
S &= \pi d^2/4, \text{reference area} \\
C_{M_\alpha} &= \text{aerodynamic pitching moment coefficient}
\end{aligned}$$

For the card material, a nondimensional overturning moment can be defined, similarly as for, M when the Equation (3) is developed:

$$M_c \equiv \frac{\rho_c S d^3}{2I_y} C_{M_{\alpha_c}}. \tag{4}$$

The corresponding nondimensional impulse for the overturning moment is obtained from Equation (2) and the transformation of the accompanying Dirac delta function (Dennery and Kryzwicki 1967), as

$$\mathcal{I}_c = \frac{\rho_c S d^2 \tau_c}{2I_y} C_{M_{\alpha_c}} \tag{5}$$

For the yaw card range, the yaw card interactions must be added to Equation (3). As discussed before, each yaw card transmits an overturning moment to the projectile which

can be modeled as an impulse located at the position s_j, which is the arclength traveled by the projectile, given in calibers. The Dirac delta function (Dennery and Kryzwicki 1967) is used with the pitching moment impulse value and the interactions of these yaw cards with a projectile are represented by replacing M with $M + \mathcal{I}_c \sum_{j=1}^{n} \delta(s - s_j)$. Equation (3) is replaced with,

$$\tilde{\xi}'' - iP\tilde{\xi}' - [M + \mathcal{I}_c \sum_{j=1}^{n} \delta(s - s_j)]\tilde{\xi} = 0. \tag{6}$$

The projectile also loses velocity when passing through each yaw card. The defining equation for P depends inversely upon the velocity, V, and so P should increase discontinuously by P_c when the projectile transits through a yaw card. The magnitude change upon the motion of the projectile can be explored by transforming Equation (6) to a form with no first derivative of the function being present (Dennery and Kryzwicki 1967),

$$\eta'' + \left(\frac{P^2}{4} + \frac{i}{2}\frac{dP}{ds} + \frac{iP_c}{2} \sum_{j=1}^{n} \delta(s - s_j) - M - \mathcal{I}_c \sum_{j=1}^{n} \delta(s - s_j) \right) \eta = 0, \tag{7}$$

in which the derivative of P is integrated across the card to obtain P_c. The value for the change in velocity in going through the card is obtained from the drag equation. With P varying inversely with the velocity, V, it is obtained that

$$P_c = \frac{\rho_c S \tau_c C_{D_c}}{2m} P \tag{8}$$

in which C_{D_c} is the projectile drag coefficient for the card medium and m is the mass of the projectile. The ratio of P_c to $\mathcal{I}_c$ yields

$$\frac{P_c}{\mathcal{I}_c} = \frac{I_x}{2md^2} \frac{pd}{V} \frac{C_{D_c}}{C_{M_{\alpha_c}}} \tag{9}$$

The first two groups on the right-hand side of Equation (9) are both much less than one, so that the change in P caused by the projectile transit through the yaw card may be neglected. One can also examine the observed phase shift because of the linear deceleration of the projectile. The observed phase shift is caused by the actual linear velocity being smaller than the expected velocity because of projectile deceleration by the cards. The calculated phase shift for a yaw card range in a normal setup configuration is much less than the phase shift generated from the pitching moment considerations. The observed phase shift from projectile deceleration through the yaw card range will therefore be neglected.

4. DIFFERENCE EQUATIONS FOR THE DIRAC DELTA APPROACH

The solution of Equation (6) in the interval between the jth card and the jth + 1 card is as given by an extension to Murphy's notation (1963):

$$\tilde{\xi} = K_{1,j}\exp(i\phi_{1,j})\exp(i\phi_1' s) + K_{2,j}\exp(i\phi_{2,j})\exp(i\phi_2' s), \tag{10}$$

in which $\phi_{1,j}$ and $\phi_{2,j}$ are the phase angles after interaction with the jth yaw card but before interaction with the jth + 1 yaw card. To conform to standard notation (Murphy 1963), $j = 0$ for projectile travel before the first yaw card is encountered. With no yaw cards, the initial phase angles, $\phi_{1,0}$ and $\phi_{2,0}$, would be constant throughout the flight. Likewise, $K_{1,j}$ and $K_{2,j}$ are the fast modal arm and slow modal arm amplitudes, respectively, after interaction with the jth yaw card but before interaction with the jth + 1 yaw card.

Now define

$$\mathcal{K}_{1,j} \equiv K_{1,j}\exp(i\phi_{1,j}), \tag{11}$$

$$\mathcal{K}_{2,j} \equiv K_{2,j}\exp(i\phi_{2,j}). \tag{12}$$

With the above definitions, Equation (10) becomes

$$\tilde{\xi} = \mathcal{K}_{1,j}\exp(i\phi_1' s) + \mathcal{K}_{2,j}\exp(i\phi_2' s). \tag{13}$$

Equation (6) can be integrated across the jth card to obtain

$$\tilde{\xi}(s_{j+}) = \tilde{\xi}(s_{j-}), \tag{14}$$

$$\tilde{\xi}'(s_{j+}) - \tilde{\xi}'(s_{j-}) = \mathcal{I}_c\tilde{\xi}(s_j). \tag{15}$$

The negative sign denotes the side that the projectile approaches and the plus sign denotes the side that the projectile leaves. Equation (13) and its derivative with respect to s can be substituted into the above difference equations for the jth + 1 card and solved for $\mathcal{K}_{k,j+1}$ in terms of $\mathcal{K}_{k,j}$, in which $k = 1, 2$:

$$\mathcal{K}_{1,j+1} = \mathcal{K}_{1,j} - \frac{i\mathcal{I}_c}{\phi_1' - \phi_2'}\mathcal{K}_{1,j} - \frac{i\mathcal{I}_c}{\phi_1' - \phi_2'}\mathcal{K}_{2,j}\exp[-i(\phi_1' - \phi_2')s_{j+1}], \tag{16}$$

$$\mathcal{K}_{2,j+1} = \mathcal{K}_{2,j} + \frac{i\mathcal{I}_c}{\phi_1' - \phi_2'}\mathcal{K}_{2,j} + \frac{i\mathcal{I}_c}{\phi_1' - \phi_2'}\mathcal{K}_{1,j}\exp[i(\phi_1' - \phi_2')s_{j+1}]. \tag{17}$$

We define that

$$\mu \equiv \frac{\mathcal{I}_c}{\phi_1' - \phi_2'}, \tag{18}$$

$$S_j \equiv (\phi_1' - \phi_2')s_j, \tag{19}$$

so that

$$\mathcal{K}_{1,j+1} = \mathcal{K}_{1,j} - i\mu\mathcal{K}_{1,j} - i\mu\mathcal{K}_{2,j}\exp(-iS_{j+1}), \tag{20}$$

$$\mathcal{K}_{2,j+1} = \mathcal{K}_{2,j} + i\mu\mathcal{K}_{2,j} + i\mu\mathcal{K}_{1,j}\exp(iS_{j+1}). \tag{21}$$

The last terms in Equations (20) and (21) contribute a phase addition that can be any sign depending on the spacing between the cards. However, the second terms in the equations show that the phase of the fast arm $\mathcal{K}_{1,j+1}$ is systematically delayed proportional to the magnitude of the perturbation, μ, whereas the phase of the slow arm, $\mathcal{K}_{2,j+1}$, is advanced proportional to the perturbation, μ. Essentially, the amount of perturbation given the epicyclic trajectories depends on the impulse moment divided by the gyroscopic stability of the projectile as given by the value of $\phi_1' - \phi_2'$. Henceforth, μ will be called the impact stability parameter.

The square of the moduli of $\mathcal{K}_{1,j+1}$ and $\mathcal{K}_{2,j+1}$ can be immediately obtained from Equations (20) and (21).

$$\left(\frac{K_{1,j+1}}{K_{1,j}}\right)^2 = 1 - 2\mu\frac{K_{2,j}}{K_{1,j}}\sin(S_{j+1} + \hat{\phi}_j) + \mu^2[1 + (\frac{K_{2,j}}{K_{1,j}})^2 + 2\frac{K_{2,j}}{K_{1,j}}\cos(S_{j+1} + \hat{\phi}_j)], \tag{22}$$

$$\left(\frac{K_{2,j+1}}{K_{2,j}}\right)^2 = 1 - 2\mu\frac{K_{1,j}}{K_{2,j}}\sin(S_{j+1} + \hat{\phi}_j) + \mu^2[1 + (\frac{K_{1,j}}{K_{2,j}})^2 + 2\frac{K_{1,j}}{K_{2,j}}\cos(S_{j+1} + \hat{\phi}_j)], \tag{23}$$

in which

$$\hat{\phi}_j \equiv \phi_{1,j} - \phi_{2,j}. \tag{24}$$

The card-induced phase angle change can be found from

$$\mathcal{K}_{1,j}^*\mathcal{K}_{1,j+1} - \mathcal{K}_{1,j}\mathcal{K}_{1,j+1}^* = 2iK_{1,j}K_{1,j+1}\sin(\phi_{1,j+1} - \phi_{1,j}), \tag{25}$$

$$\mathcal{K}_{2,j}^*\mathcal{K}_{2,j+1} - \mathcal{K}_{2,j}\mathcal{K}_{2,j+1}^* = 2iK_{2,j}K_{2,j+1}\sin(\phi_{2,j+1} - \phi_{2,j}), \tag{26}$$

in which the complex conjugate of the quantity is designated by the superposed asterisk. Performing the algebraic operations, the explicit expression for the sine of the angle change is

$$\sin(\phi_{1,j+1} - \phi_{1,j}) = \frac{-\mu[K_{1,j} + K_{2,j}\cos(S_{j+1} + \hat{\phi}_j]}{K_{1,j+1}}, \tag{27}$$

$$\sin(\phi_{2,j+1} - \phi_{2,j}) = \frac{\mu[K_{2,j} + K_{1,j}\cos(S_{j+1} + \hat{\phi}_j)]}{K_{2,j+1}}. \tag{28}$$

The encounter of the projectile will result in the delay of the fast arm phase while advancing the slow arm phase. No approximations involving the magnitude of perturbations have so far been made.

5. SOLUTION FOR SMALL PERTURBATIONS

Yaw cards are usually designed to minimize impulsive interactions with projectiles in order to obtain the best flight coefficient data possible. The yaw cards are usually placed in groups of equal distance intervals and close enough together to obtain detailed data for analysis. For an individual encounter with most yaw cards, the expressions for the moduli of the arms can be approximated in series form when $\mu K_{2,j}/K_{1,j} << 1$ and $\mu K_{1,j}/K_{2,j} << 1$:

$$\frac{K_{1,j+1}}{K_{1,j}} \approx 1 - \mu\frac{K_{2,j}}{K_{1,j}}\sin(S_{j+1} + \hat{\phi}_j) + \frac{\mu^2}{2}[1 + \frac{K_{2,j}}{K_{1,j}}\cos(S_{j+1} + \hat{\phi}_j)]^2, \tag{29}$$

$$\frac{K_{2,j+1}}{K_{2,j}} \approx 1 - \mu\frac{K_{1,j}}{K_{2,j}}\sin(S_{j+1} + \hat{\phi}_j) + \frac{\mu^2}{2}[1 + \frac{K_{1,j}}{K_{2,j}}\cos(S_{j+1} + \hat{\phi}_j)]^2. \tag{30}$$

The two modal arms can systematically grow with certain values of card spacing, the rate of growth depending upon the magnitudes of μ and $K_{1,j}/K_{2,j}$. The behavior of the amplitude values for the modal vectors of a projectile transiting a series of equally spaced cards is not obvious from examining the equations.

Taking a series solution in terms of the angle differences of the sine functions for Equations (27) and (28), it is obtained that

$$\begin{aligned}\phi_{1,j+1} - \phi_{1,j} \approx\ & -\mu[1 + \frac{K_{2,j}}{K_{1,j}}\cos(S_{j+1} + \hat{\phi}_j)] - \\ & \mu^2\frac{K_{2,j}}{K_{1,j}}[1 + \frac{K_{2,j}}{K_{1,j}}\cos(S_{j+1} - \hat{\phi}_j)]\sin(S_{j+1} + \hat{\phi}_j),\end{aligned} \tag{31}$$

$$\begin{aligned}\phi_{2,j+1} - \phi_{2,j} \approx\ & \mu[1 + \frac{K_{1,j}}{K_{2,j}}\cos(S_{j+1} - \hat{\phi}_j)] + \\ & \mu^2\frac{K_{1,j}}{K_{2,j}}[1 + \frac{K_{1,j}}{K_{2,j}}\cos(S_{j+1} + \hat{\phi}_j)]\sin(S_{j+1} + \hat{\phi}_j).\end{aligned} \tag{32}$$

The approximation will be sufficient for most yaw cards considered. For instance, μ for the problem that will addressed in this report is approximately 0.1.

When the yaw cards are read, enough information may be available to obtain acceptable data in spite of the noise generated by the trigonometric terms. If the noise can be effectively averaged, then Equations (31) and (32) become, with the defining Equation (18),

$$\phi_{1,j+1} \approx \phi_{1,j} - \frac{\mathcal{I}_c}{\phi_1' - \phi_2'} \tag{33}$$

$$\phi_{2,j+1} \approx \phi_{2,j} + \frac{\mathcal{I}_c}{\phi_1' - \phi_2'}. \tag{34}$$

Now suppose that the yaw cards are spaced apart a distance, d_c/d, in dimensions of calibers. Then, when the yaw cards are measured, the apparent values for the phase angular

rates, $\phi'_{1(R)}$ and $\phi'_{2(R)}$, with the relationship, $\mathcal{I}_c = M_c\tau_c/d$, being used is expressed as,

$$\phi'_{1(R)} = \phi'_1 - \frac{M_c\tau_c}{(\phi'_1 - \phi'_2)d_c} \tag{35}$$

$$\phi'_{2(R)} = \phi'_2 + \frac{M_c\tau_c}{(\phi'_1 - \phi'_2)d_c} \tag{36}$$

Now in terms of ϕ'_1 and ϕ'_2, it is shown (Murphy 1963) that

$$\phi'_1 = \frac{1}{2}(P + \sqrt{P^2 - 4M}), \tag{37}$$

$$\phi'_2 = \frac{1}{2}(P - \sqrt{P^2 - 4M}). \tag{38}$$

Thus,

$$\phi'_1 - \phi'_2 = \sqrt{P^2 - 4M}, \tag{39}$$

$$\phi'_1\phi'_2 = M. \tag{40}$$

So substituting Equations (37), (38), and (39) into Equations (35) and (36), the following equations are obtained:

$$\phi'_{1(R)} = \frac{1}{2}P + \frac{1}{2}\sqrt{P^2 - 4M}\left[1 - \frac{2M_c\tau_c}{(P^2 - 4M)d_c}\right], \tag{41}$$

$$\phi'_{2(R)} = \frac{1}{2}P - \frac{1}{2}\sqrt{P^2 - 4M}\left[1 - \frac{2M_c\tau_c}{(P^2 - 4M)d_c}\right]. \tag{42}$$

By multiplying the expressions for the fast arm rate and the slow arm rate together, it is obtained that the apparent value of M, $M_{(R)}$, is to the same level of approximation made in Equations (33) and (34):

$$\phi'_{1(R)}\phi'_{2(R)} \equiv M_{(R)},$$

$$= M + \frac{M_c\tau_c}{d_c}. \tag{43}$$

From Equations (3) and (4),

$$C_{M_{\alpha(R)}} = C_{M\alpha} + \tilde{D}_c C_{M_{\alpha_c}}, \tag{44}$$

in which

$$\tilde{D}_c \equiv \frac{\rho_c\tau_c}{\rho d_c}. \tag{45}$$

The apparent values of the angular velocities from the range would become

$$\phi'_{1(R)} = \frac{1}{2}P + \frac{1}{2}\sqrt{P^2 - 4[M + (M_c\tau_c)/d_c]}, \tag{46}$$

$$\phi'_{2(R)} = \frac{1}{2}P - \frac{1}{2}\sqrt{P^2 - 4[M + (M_c\tau_c)/d_c]}. \tag{47}$$

Equation (44) shows that the pitching moment data obtained from a yaw card range differ from spark range data, depending upon the density index and the card-pitching moment coefficient. The correction can be obtained from yaw card ranges by obtaining data with different values of $\tilde{D}_c$. The pitching moment coefficients obtained in a yaw card range, when plotted versus the density index, can be extrapolated back to the value for $\tilde{D}_c = 0$ to obtain the expected spark range value. The slope of the line is the card-pitching moment, $C_{M_{a_c}}$. McCoy (1993) obtained these card-pitching moment coefficients for a few projectiles, and when extrapolated back to $\tilde{D}_c = 0$, the values differed from the spark range values by less than 2%.

McCoy also extended the above formulation to stability analysis. He assumed that the above analysis could be extended to the criteria for gyroscopic stability for a statically unstable projectile, which then becomes

$$S_g = \frac{P^2}{4(M + M_c\tau_c/d_c)} > 1. \tag{48}$$

According to Equation (48), the projectile will exhibit instability when the denominator becomes larger than the numerator, which will occur with a sufficiently dense yaw card array. The flight through such an unstable configuration will be calculated with the Dirac delta model.

6. DETAILED INTERACTIONS AND COMPARISON WITH EXPERIMENT (7.62-mm RIFLE)

With the Dirac delta approach, the fluctuation and possible growth of the modal arms and phase angles can be computed in detail. The general equations can be coded and an iterative procedure used to calculate the modal arm amplitudes and phase changes caused by interaction with the yaw cards. In these calculations, no small perturbation simplifications are used. The projectile physical properties and flight coefficient parameters used for the 30-caliber test results of Hitchcock (1942) and the spark range tests of McCoy (1988) for the 7.62-mm projectile, together with the card-pitching moment coefficient calculated by McCoy (1992), are used. These parameters are

$$\begin{aligned} m &= 0.0112\,kg. \\ d &= 7.82 \cdot 10^{-3}\ \text{m}, \\ I_x &= 0.72\ \text{g} - \text{cm}^2, \\ I_y &= 6.86\ \text{g} - \text{cm}^2, \\ \frac{pd}{V} &= 0.18\ \text{rad/cal}, \end{aligned}$$

$$
\begin{aligned}
\rho &= 1.25\,\mathrm{kg/m^3}, \\
\rho_c &= 1041\,\mathrm{kg/m^3}, \\
\tau_c &= 1.65 \cdot 10^{-4}\,\mathrm{m}, \\
C_{M_\alpha} &= 2.39, \\
C_{M_{\alpha_c}} &= 3.8,
\end{aligned}
$$

These values were used to calculate what one might measure if a yaw card range were placed with equal spacing. Values for these calculated angular rates for the fast modal arm are shown in Figure 1. The yaw vectors are assumed to have equal magnitudes, a condition that is usually approximately satisfied for distances short enough that the yaw damping is negligible. For the earlier projectile-card interactions, the fluctuations are large compared to the later interactions, but the total fluctuations are less than 1% of the average value, which indicates that such a large number of cards might not be needed in an actual yaw card range. These calculated values are referenced to the first yaw card position. The distance between each calculated point is the card spacing in calibers and is equivalent to a sparse card spacing ($\tilde{D}_c = 0.061$) used by Hitchcock (1942). The earlier points calculated are not shown since, if plotted, the vertical scale showing the present plotted points would have to be greatly compressed. The observed fluctuations in the first part of the range are large compared to the fluctuations for the later points, as would be expected.

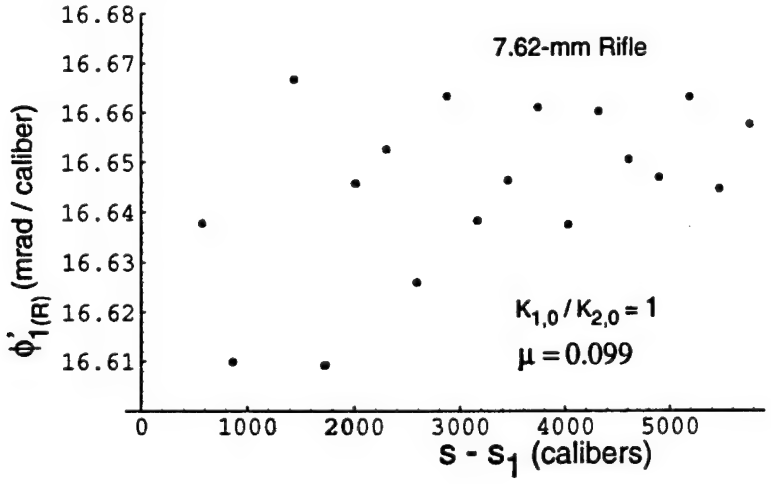

Figure 1. Calculated Range Values for the Fast Arm Velocity with Sparse Spacing.

The angular rate for the slow modal arm is shown in Figure 2. Again, the earlier calculated points are not shown. The off-scale points calculated are a consequence of starting

with the values $\phi_{1,0}$, $\phi_{2,0}$, and S_o being set equal to zero, which yields the maximum value for the fluctuation.

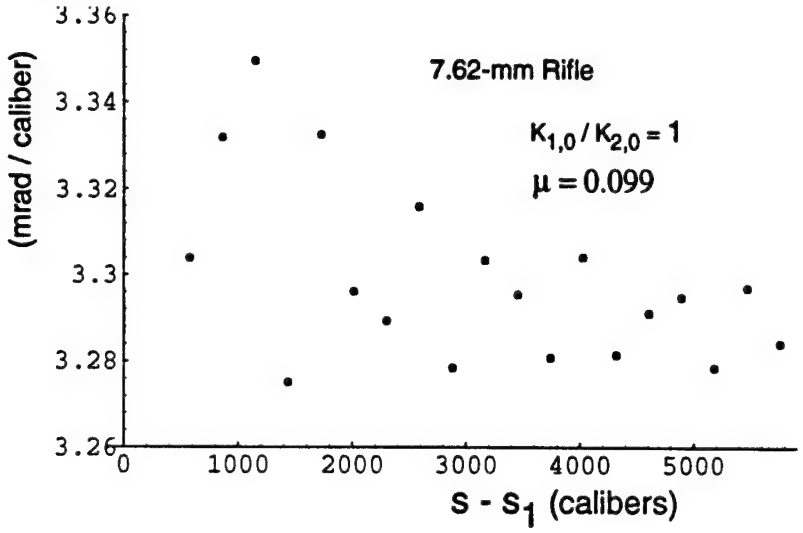

Figure 2. Calculated Range Values for the Slow Arm Velocity with Sparse Spacing.

The fast and slow arm rates were calculated for a denser yaw card array ($\tilde{D}_c = 0.15$) used by Hitchcock (1942). The fast arm results are shown in Figure 3.

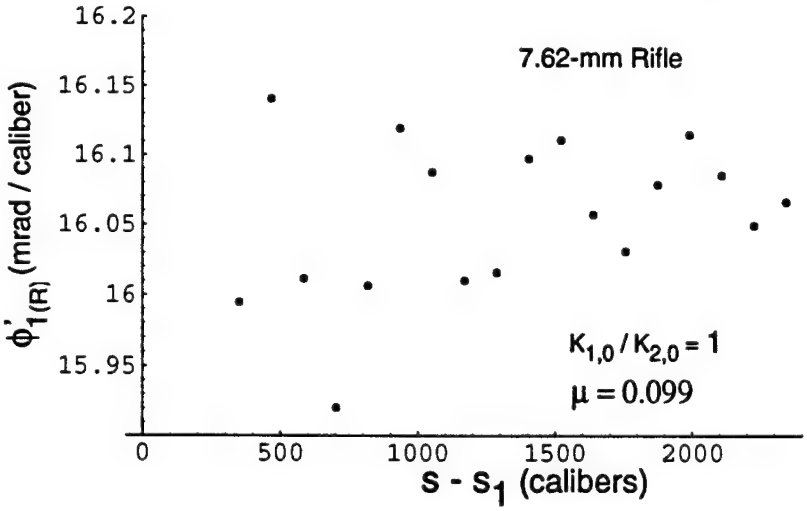

Figure 3. Calculated Range Values for the Fast Arm Velocity with Dense Spacing.

The slow arm results are shown in Figure 4. The larger fluctuations occur for the slow arm. The results from the preceding figures show expected fluctuations to less than approximately 2%, which agrees with the accuracy obtained by McCoy (1992).

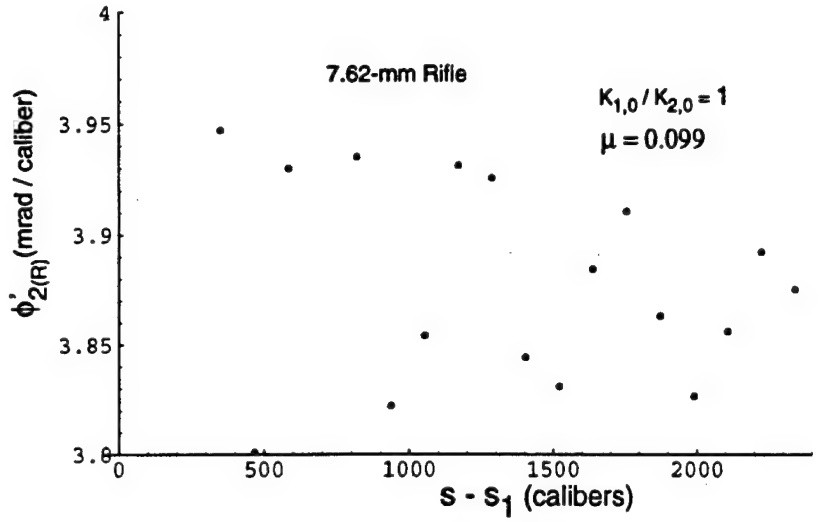

Figure 4. Calculated Range Values for the Slow Arm Velocity with Dense Spacing.

The results from the prior figures can be compared with the first approximation results as given by Equations (46) and (47), which are also the results obtained by McCoy. These results are shown in Table 1 together with results obtained when $K_{1,0}/K_{2,0} = 0.443$ and $K_{1,0}/K_{2,0} = 2.26$. The results obtained by the point-by-point calculations are only rough estimates of the modal rates because of the fluctuation magnitude.

Table 1. Calculated Range Values for Fast and Slow Arm Velocities (mrad/caliber), $\mu = 0.099$.

7.62 Rifle $\phi'_1 = 17$ mrad / caliber $\phi'_2 = 2.942$ mrad / caliber	Sparse $\tilde{D}_c = 0.061$		Dense $\tilde{D}_c = 0.15$	
	$\phi'_{1(R)}$	$\phi'_{2(R)}$	$\phi'_{1(R)}$	$\phi'_{2(R)}$
Detailed Calculations, $K_{1,0}/K_{2,0} = 0.443$	16.65	3.29	16.05	3.84
Detailed Calculations, $K_{1,0}/K_{2,0} = 1.00$	16.66	3.29	16.08	3.86
Detailed Calculations, $K_{1,0}/K_{2,0} = 2.26$	16.65	3.34	16.09	4.00
Approximation Equations (46), (47)	16.65	3.30	16.09	3.85

The amplitude change of the modal arms can also be examined in the point-by-point calculations. Figure 5 shows the net fluctuations around the original fast arm amplitude value, $K_{1,0}$, as the projectile traverses 50 cards instead of the 21 cards used previously.

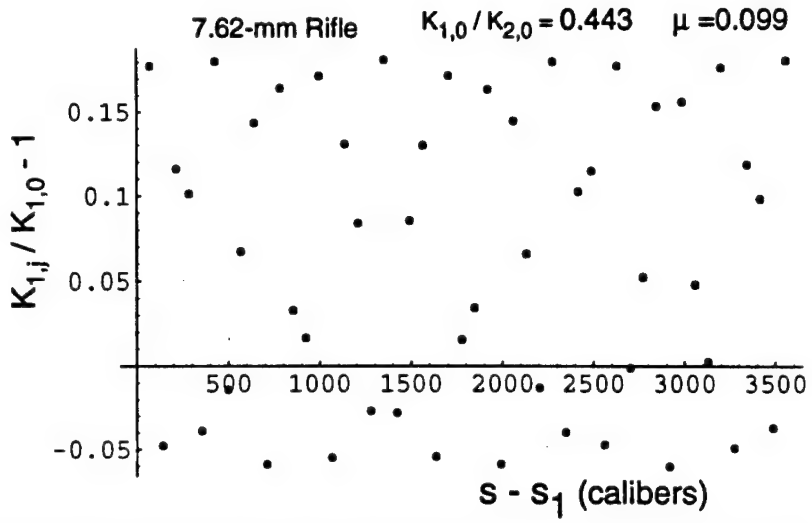

Figure 5. Net Fluctuations of Fast Arm in a Long Sparse Range ($K_{1,0}/K_{2,0} = 0.443$).

It appears that the fast arm amplitude values are oscillating about a value that is somewhat larger than the original fast arm amplitude. The average amplitude level is determined by the initial yaw values for the first projectile-card interaction. The envelope for the fluctuations is also well defined and approximates $\mu K_{2,0}/K_{1,0}$. The nonperturbed phase difference between the cards is $(\phi_1' - \phi_2')d_c/d = 4.05$.

Figure 6 shows the fractional change in the slow arm amplitude as the projectile traverses the yaw card range. The envelope of the fluctuations is much less than for the fast arm and approximates the value $\mu K_{1,0}/K_{2,0}$.

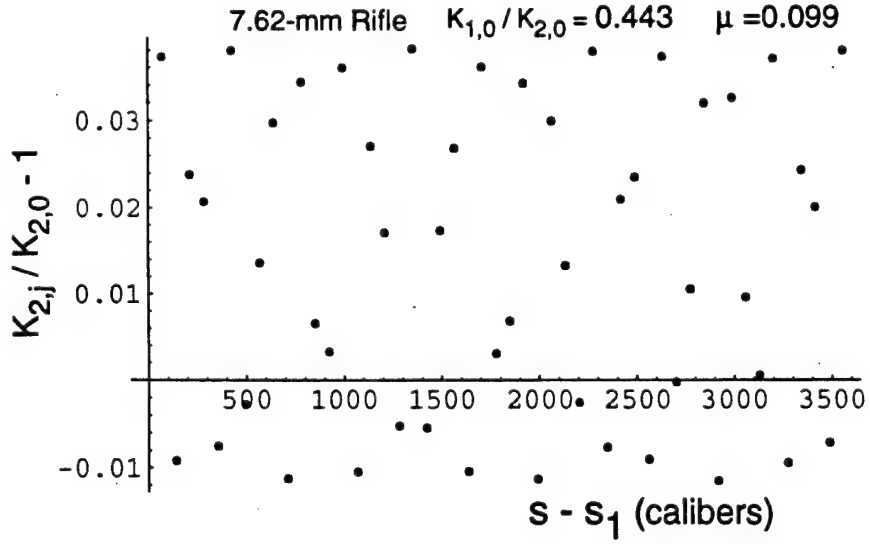

Figure 6. Net Fluctuations of Slow Arm in a Long Sparse Range ($K_{1,0}/K_{2,0} = 0.443$).

Figure 7 shows the fractional change in the fast arm amplitude as the projectile traverses a dense yaw card range. Here, the average level is decreased from the original yaw amplitude level. The initial yaw angle for the 0th iteration is 0, but other values of initial yaw angles will yield different average yaw values.

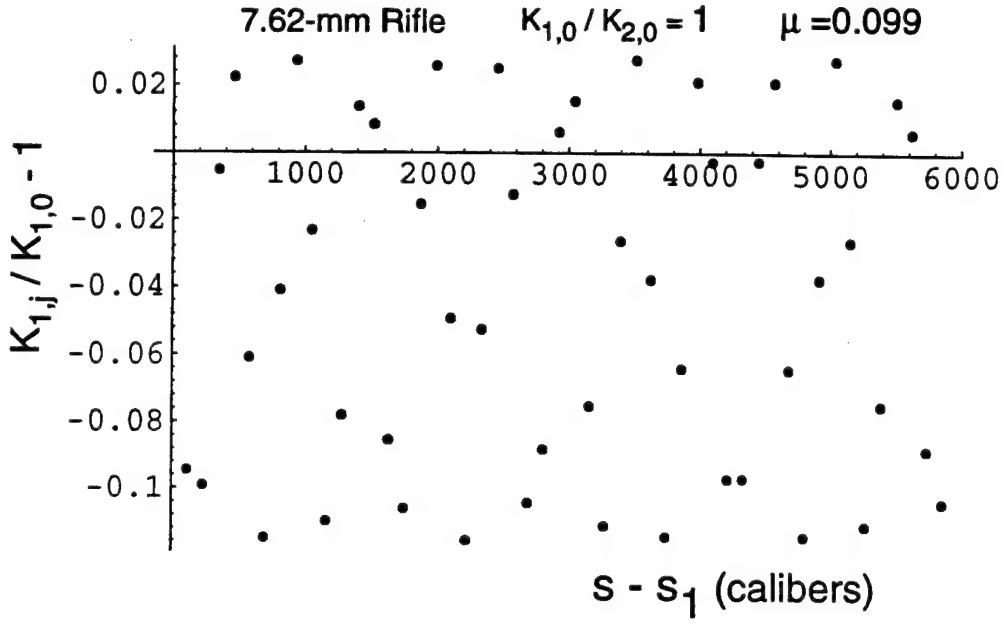

Figure 7. Net Fluctuations of Fast Arm in a Long Dense Range ($K_{1,0}/K_{2,0} = 1$).

7. CARD PLACEMENT TO INCREASE YAW

As seen in the prior section, for the distances between the cards used in Hitchcock's tests (1942), the magnitude of the yaw arms fluctuates about an average level that is near the initial yaw arm magnitude. With the yaw cards placed at selected spacings, the yaw of the projectile can be induced to grow or decline rapidly. For instance, to increase yaw at a near maximal rate, the cards would be placed so that the argument of the sine, $S_{j+1} + \hat{\phi}_j$, for Equations (22) and (23) would be $(4n+3)\pi/2$ in which n is an integer. The distance between cards to achieve the maximum amplitude gain for small μ is, using Equations (27) and (28),

$$S_{j+1} - S_j = 2\pi + 2\mu. \tag{49}$$

With μ known and the amplitudes of the modal arms being approximately equal, the phase change from a card encounter is known and unchanging. The distance between each card can then easily be calculated to maximize growth or decay of the modal arm amplitudes if the modal arm rates in ambient air are known. Calculations can also be made with the projectile entering the yaw card range at less than optimal encounter phases. Figure 8 shows

the amplitude gain for projectiles entering the yaw card range with different phase values. As before, these are the results with 7.62-mm ammunition and the use of the photographic paper referred to earlier.

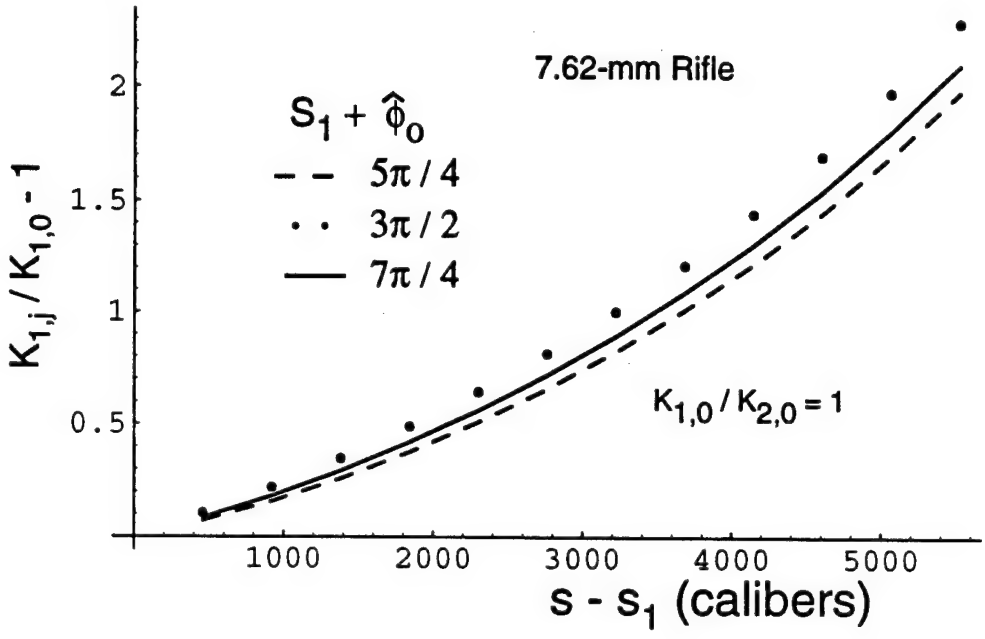

Figure 8. Net Growth of Fast Arm in Resonance Range ($K_{1,0}/K_{2,0} = 1$).

To achieve a condition for yaw arm amplification, the distance between yaw cards would have to be increased by approximately one and one-half times that for the sparse card distribution discussed earlier. Figure 8 shows that near maximum amplitude gains can be achieved even if the initial phase differs by $\pi/4$ from the phase value that yields maximum amplification or the best resonance condition. As the projectile traverses the cards, $S_{j+1} + \hat{\phi}_j$ approaches the optimal phase value, $2j\pi + 3\pi/2$. For spin-stabilized projectiles, this particular configuration will henceforth be called the yaw amplification with resonance (YAWR) range.

The approach of the encounter phase values, $S_{j+1} + \hat{\phi}_j$, to the values that would give maximum amplification with transit through a YAWR range is shown in Figure 9 when the initial encountering phase is $\pi/4$ from the optimum phase value for amplification. This behavior extends for all encounter phase values and for the slow modal arm also. The YAWR range can be thought not only as amplifying the yaw and pitch but also as a way to lock the phase of the projectile as it exits the range. This feature would make it convenient to place cameras at specified points to look for certain phenomena.

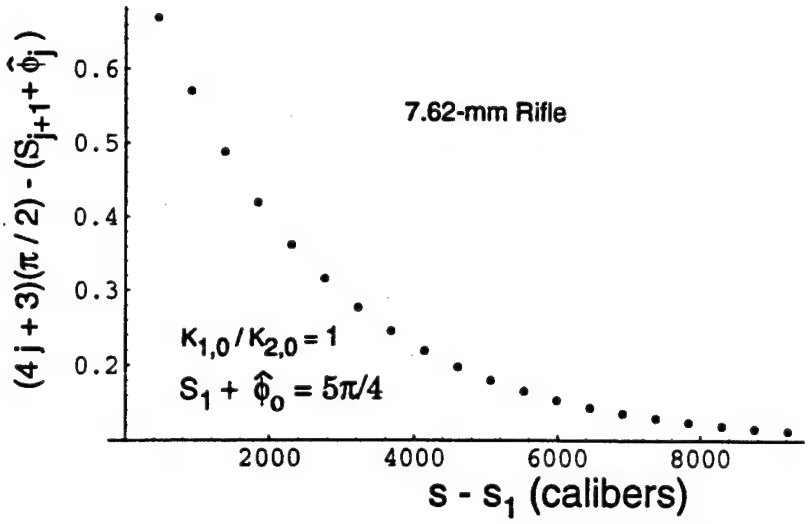

Figure 9. Approach of Encounter Phase to Optimal Value for Modal Arm Amplification in YAWR Range.

Figure 10 shows how the modal arm amplitudes may decline and then start growing in a YAWR range when the yaw card is encountered with a phase that is far away from the optimum phase for amplification. The projectile encounters the first card at such a phase value that the amplitudes diminish after passing through the yaw card. Nevertheless, the encounter phase values will approach the optimum phase value for amplitude amplification as the projectile transits the YAWR range. The card spacing necessary to achieve amplification does not need to be precise. Calculations have been done at a spacing near but not at the resonance spacing and almost as much amplification was achieved.

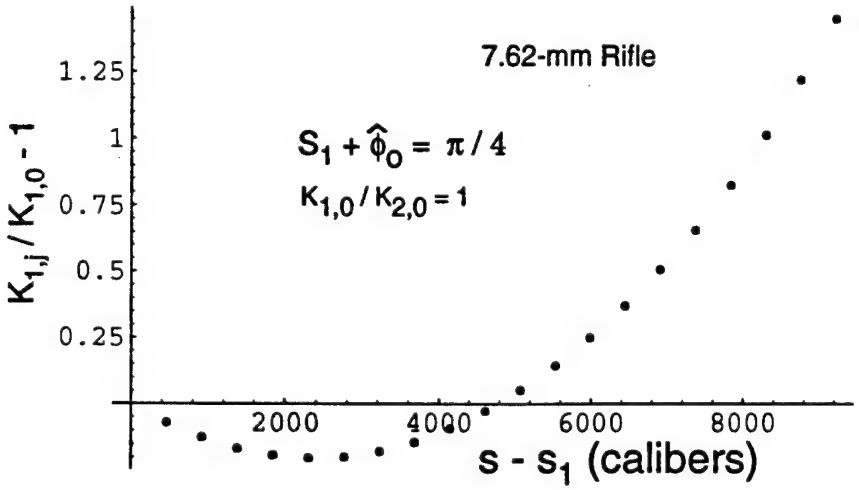

Figure 10. Net Growth of Fast Arm in YAWR Range with Initial Encounter Phase Value Set to Reduce Amplitudes.

The above figures are for the amplitude of the fast modal arm and the slow modal arm being equal, but amplitude ratios other than one can occur, especially at longer distances from the gun. Figure 11 shows the amplitude increase for the fast modal arm, in which $K_{1,0}/K_{2,0} = 0.443$.

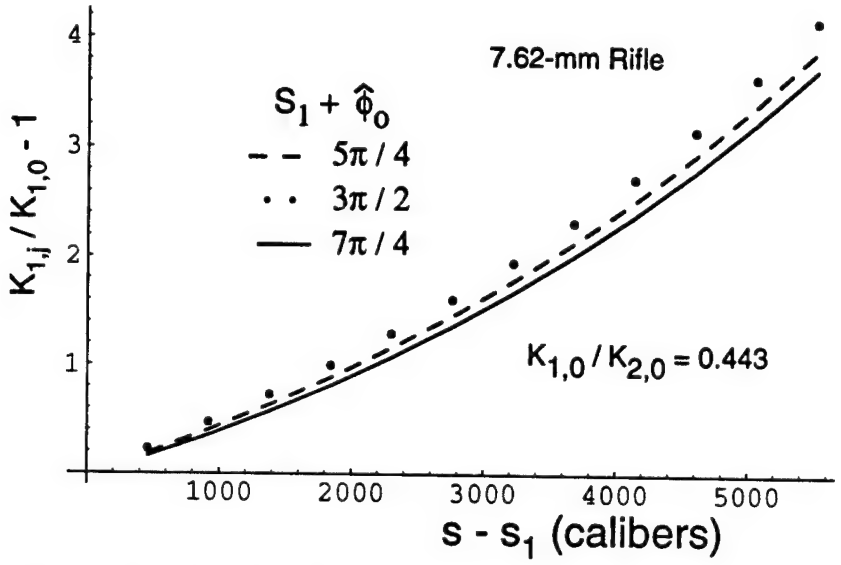

Figure 11. Net Growth of Fast Arm in YAWR Range ($K_{1,0}/K_{2,0} = 0.443$).

Again, the curves vary little with the value of the initial encounter phases shown. The fast modal arm increases rapidly relative to the growth of the slow modal arm, which is not shown. The YAWR range not only pushes the yawing motion toward a common spatial phase but also forces the modal arm amplitude ratios toward unity. If the drag coefficient for the yaw card material were the same as for air, the velocity degradation suffered by the projectiles passing through the yaw cards would be equivalent to passing through less than 2 meters of air. Although the drag coefficient for the material may be somewhat higher than it is for air, the velocity degradation through the range is minimal, while the increase in the lengths of the yaw modal arms is large, and the modal arm phases change toward the value for maximum increase in the arm amplitudes. The projectile's flight behavior through a YAWR range constitutes a remarkable phenomenon that can be used to advantage.

The yaw may also be increased by placing yaw cards at such small intervals that the projectile will fly in an unstable manner. For the 7.62-mm rifle with the photographic paper, it is calculated that $S_g < 1$ in Equation (48) if $\tilde{D}_c > 0.62$. Figure 12 shows the net growth of the fast modal amplitude for the 7.62-mm projectile passing through yaw cards at intervals so that $\tilde{D}_c = 0.7$.

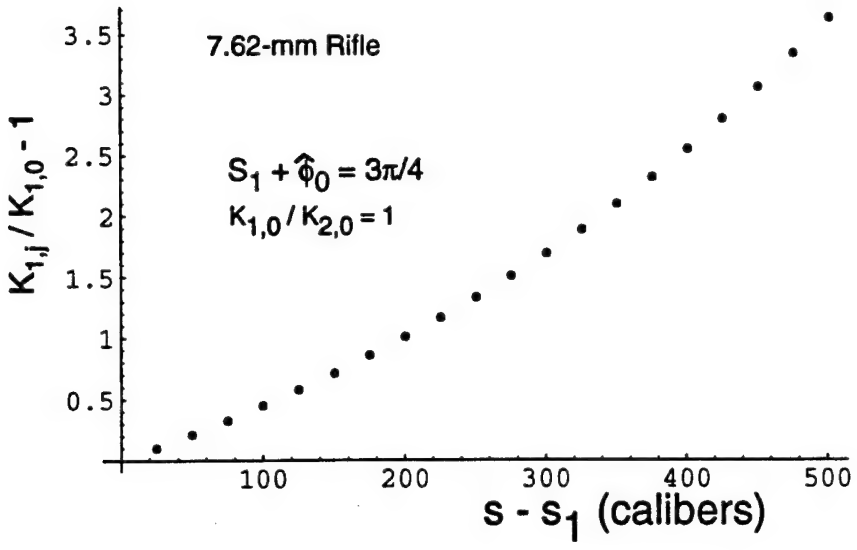

Figure 12. Fast Arm Instability Caused by Dense Range ($\tilde{D}_c = 0.7$).

For the dense unstable range conditions discussed here, the fast arm amplitude increase per encounter is less than for the YAWR range. The exact rate of growth is well predicted by a stability analysis that is being developed and will be published shortly. The stability analysis can also calculate the growth at points near the resonance condition.

8. SUMMARY AND CONCLUSIONS

The change in flight of a projectile caused by interaction with a yaw card is calculated, given its modal phase state at impact and a knowledge of the flight coefficients for the yaw card material. The impact induces both phase and amplitude changes in the modal yaw arms. The magnitude of these changes depends upon a nondimensionalized stability parameter. For chosen uniform distances between cards corresponding to stability, there is not only a fluctuation in the phase changes, but there exists a systematic decrease in the fast arm phase and a systematic gain in the slow arm phase over that observed in flight through ambient air. These systematic changes in phase are of the same order of magnitude as the fluctuating phase changes when the modal arm ratios are of the same order of magnitude. The modal arms also have fluctuation magnitudes depending on the stability parameter value. The fluctuations in both the phase and modal arm magnitudes could contribute to inaccuracies in measured values of flight coefficients.

For small values of the stability parameter, approximations to the developed flight perturbation equations can be applied to calculate modal arm rates observed from a yaw card

range with equally spaced stations. As McCoy (1992) previously showed, the modal arm rates measured in a yaw card range can be used in an extrapolation procedure to obtain flight coefficients that agree well with spark range measurements. More specifically, if testing occurs with some different series of uniform yaw card spacings and the apparent pitching moment coefficient is plotted versus the density of the different card spacings, extrapolation back to the zero value for the density of card spacings will obtain an approximate spark range value for the pitching moment coefficient.

Card placement to cause instability or increase yaw was also investigated. Instability caused by very dense spacing of cards was investigated and tends to confirm the instability criterion originally advanced by McCoy (1992). A particular configuration designed for maximum yaw growth occurs if the cards are spaced so that one period of the epicycle occurs plus a small amount more, depending on the magnitude of the stability parameter. Investigations show that the phase value for the first encounter affects the final amplification value, but the fundamental growth behavior is the same if enough cards are present. By the end of the projectile's traversal through the range, the phase value for the yaw encounters will be near the optimum value to obtain maximum growth in the modal arm amplitudes. Even though the modal arm amplitudes may be initially unequal, the resultant yawing motion at the end of a large range will be locked to a certain phase value by the processing encounters and the modal arm amplitude ratios will tend toward unity. It is anticipated that such a resonance range could be useful to induce yaw for spin-stabilized projectiles.

INTENTIONALLY LEFT BLANK.

9. REFERENCES

Boyer, E. D. "Aerodynamic Properties of the 90mm HE M-71 Shell." BRL-MR-1475, U.S. Army Ballistic Research Laboratory, Aberdeen Proving Ground, MD, April 1963. (AD 411804).

Braun, W. F. "The Free Flight Aerodynamics Range." BRL-TR-1048, U.S. Army Ballistic Research Laboratory, Aberdeen Proving Ground, MD, July 1958. (AD 411804).

Dennery, P. and A. Krzywicki. "*Mathematics for Physicists.*" Harper and Row, New York, 1967.

Hitchcock, H. P. "Stability of 90mm Shell T8." BRL-TR-236, U.S. Army Ballistic Research Laboratories, Aberdeen Proving Ground, MD, June 1941 (AD 702888).

Hitchcock, H. P. "Aerodynamics of Small Arms Bullets." BRL-TR-276, U.S. Army Ballistic Research Laboratories, Aberdeen Proving Ground, MD, May 1942 (AD 491851).

Hitchcock, H. P. "Stability of 20mm HE Shell T215E1 and T215E2." BRL-MR-655, U.S. Army Ballistic Research Laboratories, Aberdeen Proving Ground, MD, March 1953 (AD 008914).

Karpov, B. G. "A Comparison of Aerodynamic Data Obtained by 'Yaw Card' and Spark Photography Methods." BRL-MR-728, U.S. Army Ballistic Research Laboratories, Aberdeen Proving Ground, MD, October 1953 (AD 24217).

Kittyle, R. L., J. D. Packard, and G. L. Winchenbach. "Description and Capabilities of the Aeroballistic Research Facility." AFATL-TR-87-08, U.S. Air Force Armament Laboratory, Eglin Air Force Base, FL, May 1987.

McCoy, R. L. "The Aerodynamic Characteristics of 7.62mm Match Bullets." BRL-MR-3733, U.S. Army Ballistic Research Laboratories, Aberdeen Proving Ground, MD, December 1988 (AD 205633).

McCoy, R. L. "The Effect of Yaw Cards on the Pitching and Yawing Motion of Symmetric Projectiles." BRL-TR-3338, U.S. Army Ballistic Research Laboratories, Aberdeen Proving Ground, MD, May1992 (AD 205633).

McShane, E. J., J. L. Kelley, and F. V. Reno. "*Exterior Ballistics.*" The University of Denver Press, Denver, CO, 1953.

Murphy, C. H. "Free Flight Motion of Symmetric Missiles Motion of Symmetric Projectiles." BRL-TR-1216, U.S. Army Ballistic Research Laboratories, Aberdeen Proving Ground, MD, May 1963 (AD 442757).

INTENTIONALLY LEFT BLANK.

LIST OF SYMBOLS

C_{D_c}	drag coefficient for card material
C_{M_α}	aerodynamic moment overturning coefficient
$C_{M_{\alpha c}}$	moment overturning coefficient for card material
$C_{M_{\alpha(R)}}$	apparent overturning moment coefficient
d	projectile reference diameter
d_c	card spacing (m)
I_x	axial moment of inertia (kg-m^2)
I_y	transverse moment of inertia (kg-m^2
$\mathcal{I}_c$	$\frac{\rho_c S d^2 \tau_c}{2I_y} C_{M_{\alpha_c}}$, nondimensional overturning impulse for card material
$\mathcal{I}_{M_c}$	$\frac{\pi}{4}\rho_c d^3 \tau_c V C_{M_{\alpha c}} \sin\alpha_t$, card overturning moment impulse
$K_{1,j}$	fast yaw mode magnitude before transit through jth yaw card
$K_{2,j}$	slow yaw mode magnitude before transit through jth yaw card
$\mathcal{K}_{1,j}$	$K_{1,j}\exp(i\phi_{1,j})$
$\mathcal{K}_{2,j}$	$K_{2,j}\exp(i\phi_{2,j})$
m	mass of projectile
M	$\frac{\rho S d^3}{2I_y} C_{M_\alpha}$, nondimensionalized overturning moment
M_c	$\frac{\rho_c S d^3}{2I_y} C_{M_{\alpha_c}}$, nondimensionalized overturning moment for card material

M_{M_c}	$\frac{\pi}{4}\rho_c d^3 V^2 C_{M_{\alpha_c}} \sin\alpha_t$, card material overturning moment
$M_{(R)}$	apparent nondimensionalized overturning moment from card range
p	axial spin
P	$\frac{I_x}{I_y}\frac{pd}{V}$
P_c	$\frac{\rho_c S \tau_c C_{D_c}}{2m} P$, value that P decreases with transit through yaw card
s	arc length along trajectory (calibers)
S	$\pi d^2/4$, reference area
S_g	gyroscopic stability factor
S_j	$(\phi_2' - \phi_1')s_j$, total phase value to jth card
V	magnitude of velocity
α	angle of attack
α_t	total angle of attack
β	angle of side slip
η	transformed variable of ξ
μ	$\frac{\mathcal{I}_c}{\phi_1' - \phi_2'}$, impact stability parameter
ρ	air density
ρ_c	density of card material (kg / m^3)
τ_c	card thickness (m)

$\phi_{1,j}$	fast mode phase angle, between $j-1$ and jth card
$\phi_{2,j}$	slow mode phase angle, between $j-1$ and jth card
$\hat{\phi}_j$	$\phi_{1,j} - \phi_{2,j}$
$\phi'_{1(R)}$	measured fast mode angular ratefrom card range
$\phi'_{2(R)}$	measured slow mode angular rate from card range
ϕ'_1	fast mode angular rate
ϕ'_2	slow mode angular rate
$\tilde{\xi}$	$\sin\beta + i\sin\alpha$, complex yaw

INTENTIONALLY LEFT BLANK.

NO. OF
COPIES ORGANIZATION

2 ADMINISTRATOR
DEFENSE TECHNICAL INFO CENTER
ATTN DTIC DDA
8725 JOHN J KINGMAN RD STE 0944
FT BELVOIR VA 22060-6218

1 DIRECTOR
US ARMY RESEARCH LABORATORY
ATTN AMSRL CS AL TA/ RECORDS MGMT
2800 POWDER MILL ROAD
ADELPHI MD 20783-1197

1 DIRECTOR
US ARMY RESEARCH LABORATORY
ATTN AMSRL CI LL/TECH LIB
2800 POWDER MILL ROAD
ADELPHI MD 20783-1197

1 DIRECTOR
US ARMY RESEARCH LABORATORY
ATTN AMSRL CS AL TP/TECH PUB BR
2800 POWDER MILL ROAD
ADELPHI MD 20783-1197

2 DIRECTOR
US ARMY RESEARCH LABORATORY
ATTN AMSRL CI LP (TECH LIB)
BLDG 305 APG AA

No. of Copies	Organization
1	COMMANDER U S ARMY ARMAMENT MUNITIONS AND CHEMICAL COMMAND ATTN AMSMC LEP L ROCK ISLAND IL 61299-5000
1	DIRECTOR U S ARMY MISSILE & SPACE INTELLIGENCE CENTER ATTN AIAMS YDL REDSTONE ARSENAL AL 35898-5000
3	COMMANDER U S ARMY WATERVLIET ARSENAL ATTN SMCWV QAR T MCCLOSKEY SMCWV-ODW T FITZPATRICK SMCWV ODP G YARTER WATERVLIET NY 12189
1	COMMANDER US ARMY ARMAMENT RD&E CENTER ATTN AMSTA AR TD MR HIRSHMAN PICATINNY ARSENAL NJ 07801-5000
4	COMMANDER US ARMY ARMAMENT RD&E CENTER ATTN AMSTA AR AET A MR S KAHN MR M AMORUSO MR PEDERSEN MR C NG MR W TOLEDO MR B WONG PICATINNY ARSENAL NJ 07801-5000
1	COMMANDER US ARMY ARMAMENT RD&E CENTER ATTN AMSTA AR CCL D S LISS PICATINNY ARSENAL NJ 07801-5000
2	COMMANDER U S ARMY TANK AUTOMOTIVE COMMAND ATTN AMCPM BFVS AMCPM BFVS SC K PITCO WARREN MI 48397-5000
1	COMMANDER U S ARMY MISSILE COMMAND ATTN AMSMI RD DR W WALKER REDSTONE ARSENAL AL 35898-5000
1	COMMANDER TANK MAIN ARMAMENT SYSTEMS ATTN AMCPM TMA R BILLINGTON PICATINNY ARSENAL NJ 07806-5000
2	COMMANDANT U S ARMY INFANTRY SCHOOL ATTN ATSH IV SD R GORDAY ATSH TSM FORT BENNING GA 31905-5660
3	DIRECTOR BENET LABORATORIES SMCAR CCB J BENDICK SMCAR CCB DS P VOTTIS SMCAR CCB RA WATERVLIET NY 12189-4050
1	COMMANDER ARMY RESEARCH OFFICE ATTN AMXRO MCS MR K CLARK P O BOX 12211 RESEARCH TRIANGLE PARK NC 27709-2211
1	COMMANDER ARMY RESEARCH OFFICE ATTN AMXRO RT IP LIBRARY SERVICES P O BOX 12211 RESEARCH TRIANGLE PARK NC 27709-2211
1	COMMANDER AVIATION APPLIED TECHNICAL DIR ATTN SAVRT TY MSMA G MOFFATT FORT EUSTIS VA 23604-5577
3	DEPARTMENT OF THE ARMY CONSTRUCTION ENGINEERING RESEARCH LABORATORY ATTN CERL SOI P SCHOMER L PATER J WILCOSKI P O BOX 4000 CHAMPAIGN IL 61820
2	COMMANDER ASD/YHT ATTN WL/MNAA CPT J PALUMBO ASD/YHT D CURLEY EGLIN AFB FL 32542

No. of Copies	Organization
1	COMMANDER (CODE 3433) NAVAL WARFARE CENTER ATTN TECH LIB CHINA LAKE CA 93555
2	COMMANDER NAVAL SURFACE WARFARE CENTER ATTN 6X J YAGLA G MOORE DAHLGREN VA 22448
1	COMMANDER (CODE 6120C) NAVAL ORDNANCE STATION ATTN SUSAN PETERS INDIAN HEAD MD 20640
1	COMMANDER (CODE 3892) NAVAL WARFARE CENTER ATTN K SCHADOW CHINA LAKE CA 93555
1	COMMANDER (CODE 730) NAVAL SURFACE WARFARE CENTER SILVER SPRING MD 20910
1	DIRECTOR NASA SCIENTIFIC & TECHNICAL INFORMATION FACILITY ATTN SAK/DL P O BOX 8757 BALTIMORE/WASHINGTON INTERNATIONAL AIRPORT MD 21240
1	MCDONNELL DOUGLAS ATTN JOSEPH SMUCKLER 1014 FERNGATE LANE CREVE COEUR MO 63141
2	HONEYWELL COMPANY ATTN J GLASER S LANGLEY UNITED DEFENSE ARMAMENTS SYSTEM DIV 4800 EAST RIVER ROAD MINNEAPOLIS MN 55343
1	S & D DYNAMICS INC ATTN R BECKER 7208 MONTRICO DR BOCA RATON FL 33433-6930

No. of Copies	Organization
1	AAI CORPORATION ATTN T STASNEY P O BOX 126 MS 100-405 HUNT VALLEY MD 21030-0126
2	AEROJET GENERAL CORPORATION ATTN W WOLTERMAN A FLATAU P O BOX 296 AZUSA CA 91702
2	LOCKHEED AIRCRAFT INC ATTN J BROWN J PEREZ P O BOX 33 DEPT 1-330/UPLAND ONTARIO CA 91761
1	GENERAL ELECTRIC ARMAMENT & ELECTRIC SYSTEMS ATTN R WHYTE LAKESIDE AVENUE BURLINGTON VT 05401
1	FRANKLIN INSTITUTE ATTN TECH LIBRARY RACE & 20TH STREETS PHILADELPHIA PA 19103
1	THE JOHNS HOPKINS UNIVERSITY/CPIA 10630 LITTLE PATUXENT PARKWAY SUITE 202 COLUMBIA MD 21044-3200
2	LORAL CORPORATION ATTN S SCHMOTOLOCHA B AXELY 300 N HALSTEAD ST P O BOX 7101 PASADENA CA 91109
2	MCDONNELL DOUGLAS HELICOPTER CO ATTN D VAN OSTEEN R WATERFIELD MAIL STATION D216 500 E MCDOWELL RD MESA AZ 85205
1	FN MANUFACTURING INC ATTN GEORGE KONTIS POST OFFICE BOX 24257 COLUMBIA SC 29224

No. of Copies	Organization
2	ARROW TECH ASSOCIATES INC ATTN ROBERT WHYTE WAYNE HATHAWAY 1233 SHELBURNE ROAD SUITE D 8 SOUTH BURLINGTON VT 05403
1	GEORGIA INSTITUE OF TECHNOLOGY THE GEORGE W WOODRUFF SCHOOL OF MEHANICAL ENGINEERING ATTN DR G P NEITZEL ATLANTA GA 30332
1	UNITED DEFENSE L P ATTN SUZANNE DAVISON ARMAMENT SYSTEMS DIVISION 4800 EAST RIVER RD (MAIL STOP M239) MINNEAPOLIS MN 55421
1	OLD DOMINION UNIVERSITY MATHEMATICS DEPARTMENT ATTN DR CHARLIE COOKE NORFOLK VA 23508
1	SCITEC INC ATTN ALEX ZISLAN 100 WALL STREET PRINCETON NJ 08540
1	LOS ALAMOS NATIONAL LAB ATTN THOMAS DAVIS GROUP WX 4 MS G787 LOS ALAMOS NM 87545
1	OLIN CORPORATION ATTN STEPHAN FAINTICH PO BOX 222 ST MARKS FL 32355
1	ATLANTIC RESEARCH CORP ATTN MARK FRIEDLANDER 5945 WELLINGTON ROAD MS G787 GAINESVILLE VA 22065
2	UNIVERSITY OF VIRGINIA DEPARTMENT OF MECHANICAL AND AEROSPACE ENGINEERING ATTN H G WOOD III J MORTON CHARLOTTESVILLE VA 22901

No. of Copies	Organization
	Aberdeen Proving Ground
2	DIR USAMSAA ATTN AMXSY D W BROOKS R CONROY
5	CDR USAATC ATTN STECS AAL M MAULE STECS AS LA S. WALTON STECS DA P PAULES STECS RM PF S HINTE STECS AS HP J ANDREWS
2	CDR USATECOM ATTN AMSTE TE R MR KEELE AMSTE TA R W MARSHALL
1	DIR AMC INT MAT EVAL DIV ATTN AMCICP IM R BLOOM
4	DIR USAARDEC ATTN SMCAR FSF T R LIESKE J MATTS R PUHALLA J WHITESIDE FIRING TABLES BRANCH BLDG 120

No. of Copies	Organization
40	DIR USARL
	ATTN AMSRL WM
	I MAY
	AMSRL WM P
	A HORST
	E SCHMIDT
	AMSRL WM PA
	T MINOR
	G KELLER
	M NUSCA
	AMSRL WM PC R FIFER
	AMSRL WM PD B BURNS
	AMSRL WM W C MURPHY
	AMSRL WM WB
	W D'AMICO
	B DAVIS
	F BRANDON
	G BROWN
	AMSRL WM WC
	J BORNSTEIN
	R VON WAHLDE
	AMSRL WT PB
	K FANSLER (4)
	J WIDDER (3)
	P PLOSTINS
	D WEBB
	G COOPER (2)
	M BUNDY
	B PATTON
	K SOENCKSEN
	V OSKAY
	J GARNER
	P WEINACHT
	B GUIDOS
	H EDGE
	J SAHU
	A MIKHAIL
	A ZIELINSKI
	AMSRL HR SD J KALB
	AMSRL SC C C NIETUBICZ
	AMSRL SC CC A CELMINS

INTENTIONALLY LEFT BLANK.

REPORT DOCUMENTATION PAGE

Form Approved
OMB No. 0704-0188

1. AGENCY USE ONLY *(Leave blank)*	2. REPORT DATE	3. REPORT TYPE AND DATES COVERED
	January 1997	Final

4. TITLE AND SUBTITLE

Yaw Card Perturbation of Projectile Dynamics

5. FUNDING NUMBERS

PR: 1L162618AH80

6. AUTHOR(S)

Cooper, G. R.; Fansler, K. S.

7. PERFORMING ORGANIZATION NAME(S) AND ADDRESS(ES)

U.S. Army Research Laboratory
Weapons & Materials Research Directorate
Aberdeen Proving Ground, MD 21010-5066

8. PERFORMING ORGANIZATION REPORT NUMBER

9. SPONSORING/MONITORING AGENCY NAME(S) AND ADDRESS(ES)

U.S. Army Research Laboratory
Weapons & Materials Research Directorate
Aberdeen Proving Ground, MD 21010-5066

10. SPONSORING/MONITORING AGENCY REPORT NUMBER

ARL-TR-1258

11. SUPPLEMENTARY NOTES

12a. DISTRIBUTION/AVAILABILITY STATEMENT

Approved for public release; distribution is unlimited.

12b. DISTRIBUTION CODE

13. ABSTRACT *(Maximum 200 words)*

Projectile flight through a yaw card range is investigated with particular attention given to the apparent change in the flight coefficients. Encounters of the projectile with the yaw cards are treated as impulses, resulting in calculated abrupt changes in the yaw modal arms' phases and amplitudes. Further approximations are made to describe small perturbing encounters and to obtain an expression for the apparent or range value for the overturning moment coefficient. For 7.62-mm ammunition, apparent flight coefficients are calculated point by point for various yaw card spacings and compared with simple approximating expressions. Resonance conditions are also investigated, whereby the yawing motion of a spin-stabilized projectile can be amplified. These resonance conditions force the amplitude ratio for the fast and slow modal arms toward unity and the encountering phase angle of the projectile toward a value that maximizes the amplification for each encounter.

14. SUBJECT TERMS

flight mechanics; particle trajectory; yaw card; flight stability; projectile stability

15. NUMBER OF PAGES

43

16. PRICE CODE

17. SECURITY CLASSIFICATION OF REPORT	18. SECURITY CLASSIFICATION OF THIS PAGE	19. SECURITY CLASSIFICATION OF ABSTRACT	20. LIMITATION OF ABSTRACT
Unclassified	Unclassified	Unclassified	